Published in final edited form as:

Cell Transplant. 2016 November ; 25(11): 1967–1977. doi:10.3727/096368916X691457.

HIV Non-Nucleoside Reverse Transcriptase Inhibitor Efavirenz Reduces Neural Stem Cell Proliferation In Vitro and In Vivo

Jingji Jin[*], **Bethany Grimmig**[†], **James Izzo**[*], **Lecia A. M. Brown**[*], **Charles Hudson**[‡], **Adam J. Smith**[†], **Jun Tan**[†,‡,§], **Paula C. Bickford**[†,‡], and **Brian Giunta**[*]

[*]Department of Psychiatry and Behavioral Neurosciences, Neuroimmunology Laboratory, University of South Florida Morsani College of Medicine, Tampa, FL, USA

[†]Center of Excellence for Aging and Brain Repair, Department of Neurosurgery and Brain Repair, University of South Florida Morsani College of Medicine, Tampa, FL, USA

[‡]Research Service, James A. Haley VA Hospital, Tampa, FL, USA

[§]Department of Psychiatry and Behavioral Neurosciences, Rashid Laboratory for Developmental Neurobiology, University of South Florida Morsani College of Medicine, Tampa, FL, USA

Abstract

The prevalence of HIV-associated neurocognitive disorders (HAND) remains high despite combination antiretroviral therapy (cART). There is evidence that neural stem cells (NSCs) can migrate to sites of brain injury such as those caused by inflammation and oxidative stress, which are pathological features of HAND. Thus, reductions in NSCs may contribute to HAND pathogenesis. Since the HIV non-nucleoside reverse transcriptase inhibitor efavirenz (EFV) has previously been associated with cognitive deficits and promotion of oxidative stress pathways, we examined its effect on NSCs in vitro as well as in C57BL/6J mice. Here we report that EFV induced a decrease in NSC proliferation in vitro as indicated by MTT assay, as well as BrdU and nestin immunocytochemistry. In addition, EFV decreased intracellular NSC adenosine triphosphate (ATP) stores and NSC mitochondrial membrane potential (MMP). Further, we found that EFV promoted increased lactate dehydrogenase (LDH) release, activation of p38 mitogen-activated protein kinase (MAPK), and increased Bax expression in cultured NSCs. Moreover, EFV reduced the quantity of proliferating NSCs in the subventricular zone (SVZ) of C57BL/6J mice as suggested by BrdU, and increased apoptosis as measured by active caspase-3 immunohistochemistry. If these in vitro and in vivo models translate to the clinical syndrome, then a pharmacological or cell-based therapy aimed at opposing EFV-mediated reductions in NSC proliferation may be beneficial to prevent or treat HAND in patients receiving EFV.

Keywords

Neural stem cells (NSCs); Efavirenz (EFV); Oxidative stress

INTRODUCTION

Soon after infection, human immunodeficiency virus-1 (HIV-1) enters the central nervous system (CNS)[1]. Survival times with chronic HIV-1 infection continue to grow, and as a

result there is an increasingly large number of patients harboring the virus within the brain. This may be one contributing factor to the substantial prevalence of HIV-associated neurocognitive disorders (HAND), which affects up to 45% of HIV-infected patients[2].

Past reports have indicated a link between HIV-1 and reduced proliferation of neural stem cells (NSCs) as well as reduced neurogenesis[3]. Although HIV does not infect mature neurons, the virus has been shown to infect NSCs[4]. It has further been shown that the early HIV-1 infection of NSCs may lead to neurocognitive dysfunction[5,6]. Importantly, NSCs have an ability for precise migration to widespread areas of pathology in the brain[7–12]. Thus, their reduction may be a contributing factor to HAND, which is marked by chronic inflammatory and oxidative injury in the brain[13–15].

The HIV non-nucleoside reverse transcriptase inhibitor efavirenz (EFV) has been a common component of combination antiretroviral therapy (cART) for HIV infection[16,17] and has also been associated with cognitive side effects in both human clinical studies and murine models[16,18,19]. Studies on human glioma and neuroblastoma cell lines as well as rat primary cultures of neurons and astrocytes indicate the involvement of EFV in oxidative stress in the CNS[20]. EFV inhibits HIV-1 replication via several mechanisms[21], but largely by promoting conformational changes within the HIV-1 reverse transcriptase at the polymerase active site[22]. We performed these experiments to determine whether EFV could affect NSC proliferation in vitro and in vivo. We sought to understand one possible reason why cognitive disorders may occur in patients with well-controlled HIV infection who are on EFV therapy[16,18].

MATERIALS AND METHODS

All experimental procedures were approved by the Institutional Animal Care and Use Committee (IACUC) of the University of South Florida. C57BL/6J female mice (8 months old) were purchased from The Jackson Laboratory (Bar Harbor, ME, USA) and were housed in environmentally controlled conditions (12:12-h light/dark cycle at 21 ± 1°C) and provided food and water ad libitum.

Reagents

EFV was provided by the NIH AIDS Reagent Program (Germantown, MD, USA) or purchased from Sigma-Aldrich (St. Louis, MO, USA). A series of concentrations of EFV was used to determine its effect on NSC proliferation, adenosine triphostate (ATP) levels, mitochondrial membrane potential (MMP), and lactate dehydrogenase (LDH) in vitro (0.5, 1, 2, 5, and 10 μM). The dose of EFV administered in vivo (20 mg/kg) was based on the body weight of the mice, the dosing period of 30 days, as well as our[23] and other[24] previous publications.

Rat NSC Culture

Rat NSCs (cat. #SCR021; EMD Millipore, Billerica, MA, USA) were cultured in DMEM/F12 media supplemented with serum-free Neuro-27 medium (EMD Millipore), 20 ng/ml human fibroblast growth factor 2 (FGF-2; EMD Millipore), 20 ng/ml human epidermal growth factor (hEGF; PeproTech, Rocky Hill, NJ, USA), and 20 ng/ml L-

glutamine 2 mM (Life Technologies, Carlsbad, CA, USA), as well as penicillin and streptomycin 100 U/ml (Life Technologies) at 37°C in 5% carbon dioxide. Culture media were exchanged every 2 days. Ten-centimeter dishes and 96-well plates were precoated with 10 μg/ml of poly-L-ornithine (EMD Millipore), followed by laminin (EMD Millipore) at a concentration of 10 μg/ml in phosphate-buffered saline (PBS) solution. NSC treatments were performed during passages 2–6. Treatments were performed in the same medium used for cell culture.

MTT Assay

Cell viability was measured by Cell Proliferation Kit (MTT assay) (Roche, Indianapolis, IN, USA). Briefly, NSCs were plated on precoated 96-well plates at a density of 10^4 cells per well and incubated at 37°C in 5% carbon dioxide for 24 h. After treatment with a series of concentrations of EFV, vehicle control [ctrl; <0.1% dimethyl sulfoxide (DMSO; Sigma-Aldrich) in PBS], or H_2O_2 (100 μM; positive control) for 24 h, 10 μl of MTT solution (5 mg/ml) was added into each well and incubated at 37°C for 4 h. Next, 100 μl of solubilization solution (10% SDS in 0.01 M HCl) was added to each well and incubated at 37°C overnight. Optical density (OD) was detected at a wavelength of 550 nm via a microplate reader (Synergy H1; BioTek, Winooski, VT, USA). The percentages of treatment OD divided by the vehicle control OD represented the NSC proliferation value.

Proliferation of NSCs Detected by Immunocytochemistry

NSCs were grown in four-well chambered coverglass (Thermo Fisher Scientific NUNC, Rochester, NY, USA) at a density of 3×10^4 for 24 h. After exposure to 5 μM of EFV or vehicle control for 24 h, 10 μM of bromodeoxyuridine (BrdU; Sigma-Aldrich) was added at 37°C for 2 h. Next, 4% paraformaldehyde (PFA) in PBS was added to each well at room temperature (RT) for 20 min for fixation. NSCs were blocked with 3% donkey serum, incubated with mouse anti-nestin antibody (1:500; Covance, Dedham, MA, USA) at 4°C overnight, and then incubated with secondary Alexa Fluor 594 donkey anti-mouse IgG (1:200; Vector Laboratories Inc., Burlingame, CA, USA) at RT for 1 h. NSCs were treated with 2N HCl for 10 min at RT to denature DNA and were neutralized by citric acid buffer (pH 7.4; Thermo Fisher Scientific, Fair Lawn, NJ, USA) for 10 min. Cells were blocked with 3% donkey serum incubated with rat anti-BrdU antibody (1:250; Accurate Chemical & Scientific Corp., Westbury, NY, USA) at 4°C overnight, and then incubated with secondary antibody Alexa Fluor 488 donkey anti-rat IgG (1:200; Vector Laboratories Inc.) at RT for 1 h. Images were taken using an inverted IX53 microscope and a DP22 color camera (Olympus, Center Valley, PA, USA). The proliferation of NSCs was measured by the percentage of double fluorescence staining of BrdU (green) and nestin (red) over total nestin-positive cells.

Adenosine Triphosphate (ATP) Bioluminescence Assay

Quantitative intracellular ATP levels in vitro were measured using an ATP Determination Kit (Invitrogen, Carlsbad, CA, USA)[25] in strict accordance with the manufacturer's instructions. Briefly, NSCs were plated in 12-well plates at a density of 3×10^5 per well and incubated at 37°C for 24 h. After treatment with a series of concentrations of EFV (0.5, 1, 2, 5, and 10 μM), vehicle control, and positive control (H_2O_2; 100 μM) for 24 h, cells were lysed by Tris

lysis buffer (Bio-Rad, Hercules, CA, USA) on ice for 30 min and subjected to sonification for 30 s at 40% power. Next, 90 µl of the pre-mixed solution, including D-luciferin, firefly luciferase, dithiothreitol, adenosine 5′-triphosphate, and assay buffer was transferred into 96-well plates (Greiner Bio-One, Monroe, NC, USA). Afterward, 10 µl of cell lysate solution or ATP standard solutions were added into the wells with triplication. Relative luminescence units (RLU) were detected with a microplate reader (Synergy H1; BioTek). Percentages of EFV treatment over vehicle control represented intracellular ATP levels.

LDH Assay

Cell death in vitro was measured by an LDH assay kit (Thermo Fisher Scientific, Rockford, IL, USA). NSCs were plated in 96-well plates at a density of 10^4 per well for 24 h and then treated with EFV (0.5, 1, 2, 5, and 10 µM), vehicle control, and cell lysis buffer (positive control, 30 min) for 24 h at 37°C in 5% carbon dioxide. Fifty microliters of cell culture media from each treatment was transferred to a flat-bottom 96-well plate, and 50 µl of reaction mixture (supplied in kit) was added into each well and incubated at RT for 30 min. After adding stop solution, the OD at 490 nm subtracted from the OD at 680 nm represented the LDH value.

JC-1 Assay

MMP was evaluated by a JC-1 MMP detection kit (Biotium, Hayward, CA, USA). Detection was performed in strict accordance with the manufacturer's instructions. In brief, NSCs were plated in 96-well plates at a density of 10^4 cells/well at 37°C in 5% carbon dioxide for 24 h. EFV was applied at concentrations of 0.5, 1, 2, 5, and 10 µM. Vehicle control and H_2O_2 (100 µM; positive control) were also examined. After 6 h of treatment, JC-1 was added into culture media for 15 min at 37°C. JC-1 accumulated on mitochondrial membranes (nonapoptotic cells, red) or remained in the cytoplasm (apoptotic cells, green)[26]. Media were exchanged for PBS. Next, red fluorescence (RFU; excitation, 550 nm; emission, 600 nm) and green fluorescence (excitation, 485 nm; emission, 535 nm) were measured by fluorescence microplate reader (Synergy H1; BioTek). The value of red fluorescence divided by green fluorescence represented MMP.

Western Blots

Following 5 µM of EFV or vehicle control treatment, NSCs were harvested and lysed by radioimmunoprecipitation assay (RIPA) buffer in 1 mM phenylmethane sulfonyl fluoride (PMSF), protease inhibitor cocktail, and phosphatase inhibitor cocktail (Sigma-Aldrich). Protein concentrations were detected with a bicinchoninic acid (BCA) protein assay kit. Thirty to 50 µg of total protein was applied to sodium dodecyl sulfate (SDS)-PAGE (10% polyacrylamide gel) and transferred to polyvinylidene difluoride (PVDF) membranes (EMD Millipore). Blots were incubated for 1 h in 0.05% Tween 20 (Sigma-Aldrich) in Tris-buffered saline (TBS; Bio-Rad) containing 5% non-fat dry milk (Bio-Rad). After three washes with PBS in 0.05% Tween 20, membranes were incubated for 16 h with one of the following primary antibodies: phospho-p38 mitogen-activated protein kinase (MAPK) antibody (Thr180/Tyr182; Cell Signaling Technology, Danvers, MA, USA), total p38 MAPK antibody (Cell Signaling Technology), or Bax polyclonal antibody (EMD Millipore) at 4°C for 1 h with horseradish peroxidase (HRP)-conjugated secondary antibodies (diluted

2,000-fold) at RT. Target proteins were visualized using SuperSignal West Pico Chemiluminescent Substrate (Thermo Fisher Scientific). Blots were stripped and reprobed with anti-β-tubulin III (1:8,000; Covance). The resulting protein bands were scanned using an HP Laser Jet 9050 mfp System (HP Inc., Palo Alto, CA, USA), and densitometric analysis of each protein band was performed using ImageJ v1.45 (NIH, Bethesda, MD, USA). To normalize for protein loading, the densitometric analysis of each band was divided by the β-tubulin III band from the same membrane for Bax and total p38 MAPK for phospho-p38 MAPK.

Administration of EFV and Tissue Processing

Eight-month-old C57BL/6J mice were randomly divided into two groups matched by body weight and gender. One group received EFV via intraperitoneal (IP) injection at a dose of 20 mg/kg daily (eight mice) in vehicle control [5% DMSO, 17% Tween 80 (Sigma-Aldrich) in 5% glucose solution][27], while the other group received vehicle control only via IP injection (seven mice). The dose used in the present study (20 mg/kg) is in the range of those used in other studies (10–30 mg/kg) investigating various effects of EFV in rodents[24,28–31]. The injection period was 4 weeks. On the final week, mice received 50 mg/kg of BrdU (Sigma-Aldrich) in PBS via IP injection daily for 5 consecutive days. Twenty-four hours later, all mice were deeply anesthetized with 1%–2% isoflurane (Henry Schein Animal Health, Dublin, OH, USA) and transcardially perfused with 20 ml of cold PBS followed by 20 ml of 4% PFA in PBS. Mouse brain tissues were removed, postfixed with 4% PFA (pH 7.4) at 4°C for 24 h, and then neutralized with 30% sucrose in PBS (pH 7.2). Mouse brains were sectioned using a microtome (Leica, Buffalo Grove, IL, USA) at 40-μm thickness. Sagittal sections from the right hemisphere were used for immunohistochemistry (IHC) staining.

Immunohistochemistry Analysis

Sections were blocked with 5% goat serum (Thermo Fisher Scientific, Waltham, MA, USA), 2% bovine serum albumin (BSA; Thermo Fisher Scientific) in PBS, and 0.1% Triton X-100 followed by hybridization at 4°C overnight with goat anti-doublecortin antibody (Dcx; 1:200; Santa Cruz Biotechnology, Dallas, TX, USA). Sections were then washed and incubated with biotinylated anti-goat IgG antibody (1:200; Vector Laboratories). For BrdU analysis, we followed our previous protocol[32]. Briefly, sagittal sections were treated with 50% formamide (Sigma-Aldrich)/2× SSC (0.3 M NaCl, 0.03 M sodium citrate) at 65°C for 2 h, rinsed in 2× SSC, incubated in 2N HCl for 30 min at 37°C, rinsed with borate buffer (pH 8.5; Sigma-Aldrich) for 10 min, and then washed with PBS twice. Sections were incubated with rat anti-BrdU antibody (1:250; Accurate Chemical & Scientific) at 4°C overnight, and with biotinylated goat anti-rat IgG (1:200), and developed in 3,3′-diaminobenzidine (DAB) solution. After mounting the sections onto slides, quantification of positive Dcx and BrdU immunostaining in the subventricular zone (SVZ) was conducted by scanning the slides using an Axio Scan Z.1 scanner (Carl Zeiss Inc., Thornwood, NY, USA) to produce 20x digital images. Using the NearCYTE STI computer program (nearcyte.org), a researcher blind to the treatment conditions outlined the region of interest (ROI) that was then compared to a user-defined pixel color threshold. This file was applied to all of the sections to be analyzed in order to designate positive staining within the determined area. The files were batch processed to generate a ratio of positive stain to the total area for each contour

drawn on a slide image. Regarding active caspase-3 analysis, tissue sections were immunostained by free floating method. The primary antibody used was rabbit anti-active caspase-3 antibody (1:250; Sigma-Aldrich). Vectastain ABC (Vector Laboratories) and nickel DAB reagents (Sigma-Aldrich) were used to identify active caspase-3-positive cells. Sections were mounted and imaged manually using an Olympus BX51 microscope with a U-CMAD3 camera (Olympus). The images were taken by Dp 70 software (Olympus) and analyzed by ImageJ 1.47v. The entire area of the SVZ (50 fields, 0.15 mm^2 each) from three sagittal brain sections per mouse was analyzed. Each was separated by a 240 μm interval. The number of active caspase-3-positive cells per mm^2 was quantified.

Statistical Analysis

All statistical analyses were performed with SPSS software (version 18.0; IBM, Armonk, NY, USA). Data are expressed as mean ± SEM, and results were deemed significant when $p<0.05$. Variables between groups were determined by independent *t*-test or one-way analysis of variance (ANOVA). When significance was achieved, analysis of groups was performed using Tukey's post hoc test.

RESULTS

EFV Reduces Proliferation of NSCs

As shown in Figure 1A, EFV decreased cell proliferation in a concentration-dependent manner. At the 5 μM EFV concentration, there were approximately 74% of live cells compared to vehicle control ($p < 0.05$). When EFV concentration was 10 μM, live cells were detected at approximately 36% compared to vehicle control treatment ($p<0.001$). NSC proliferation had a progressive decline as EFV concentration increased. The threshold for this decline was the 5 μM concentration of EFV. As shown in Figure 1B, BrdU incorporation reflected cell proliferation, and nestin was used as an NSC marker[33]. The number of double-fluorescent-labeled cells was significantly decreased by EFV treatment compared with vehicle control. Vehicle control treatments are shown in Figure 1B: (a) BrdU, (b) nestin, and (c) merged. EFV treatment (5 μM) is shown in (d) BrdU, (e) nestin, and (f) merged; (g) quantified data expressed as percentage of double-labeled cells show significant decreases in proliferation in EFV-treated NSCs ($p <0.001$) (Fig. 1B).

EFV Reduces NSC ATP Stores and MMP

NSC viability can also be measured by ATP assay. In order to maintain biophysiologic function, intracellular ATP levels must remain consistent to maintain homeostasis. To determine if EFV could decrease ATP levels in NSCs, as shown in Figure 2A, they were treated with a series of concentrations of EFV as well as positive (H_2O_2, 100 μM) and vehicle controls for 24 h. Cell lysates were used to measure ATP levels, and 5 μM of EFV decreased ATP levels to approximately 78% of vehicle control levels ($p < 0.05$). EFV (10 μM) reduced cellular ATP stores by approximately 57% compared to that of vehicle control ($p < 0.01$) (Fig. 2A). Loss of MMP is an event associated with oxidative stress and the initiation and activation of apoptosis[26,34,35]. As shown in Figure 2B, NSCs were treated with a series of concentrations of EFV, vehicle control, and positive control (H_2O_2; 100 μM) for 6 h followed by the addition of JC-1. In healthy cells, the JC-1 reagent aggregates on intact

mitochondrial membranes and shows red fluorescence, whereas in apoptotic cells it exists in monomeric form in the cytoplasm showing green fluorescence. The value of red fluorescence (excitation, 550 nm; emission, 600 nm) divided by green fluorescence (excitation, 485 nm; emission, 535 nm) represents MMP. Similar to MTT and ATP assays, the threshold concentration was 5 μM of EFV to observe significant effects (Fig. 2B).

EFV Increases NSC Cytotoxicity and Cell Death

Because loss of mitochondrial function as examined by JC-1 can lead to apoptosis, we also examined EFV-promoted cell death by LDH assay. We again treated NSCs with a series of concentrations of EFV, vehicle control, and positive control (cell lysis buffer, 30 min) for 24 h (Fig. 3). The cell-cultured media were subjected to LDH assay. The higher the cell death, the more LDH was released into the media via cell membrane damage. EFV promoted toxic responses from NSCs in a concentration-dependent manner. EFV (5 μM) increased LDH release by nearly twofold compared with vehicle control ($p < 0.001$), while 10 μM of EFV increased LDH release by approximately threefold ($p < 0.001$).

Effect of EFV on p38 MAPK Phosphorylation and Bax Expression

It has been reported that the phosphorylation of p38 MAPK and Bax activation are central antiproliferation inducers of several cell types including stem cells[36–38]. This was evidenced by a phosphorylation of p38 in EFV-stimulated NSCs. We treated these cells with EFV (5 μM; based on the threshold concentration for significant effects on NSC mitochondrial function, proliferation, and cytotoxicity) for 1 h and found that EFV significantly enhanced phospho-p38 (Ph-p38) expression by Western blot ($p < 0.01$) (Fig. 4A). To investigate whether p38 MAPK could be correlated with upregulated Bax expression, NSCs were further treated with the same concentration of EFV for 24 h, which significantly increased Bax expression ($p < 0.05$) (Fig. 4B).

EFV Administration Impairs NSC Proliferation and Induces Apoptosis in the SVZ In Vivo

To explore NSC proliferation after EFV administration in vivo, C57BL/6J mice at 8 months of age were injected (IP) with 20 mg/kg of EFV or vehicle control for 4 weeks. During the final 5 days, mice additionally received a dose of 50 mg/kg of BrdU daily. Quantitative analysis showed that BrdU expression was significantly decreased in the EFV treatment group in the SVZ compared to the control group ($p < 0.05$) (Fig. 5A), indicating an impairment of proliferation. Figure 5B exhibits images of Dcx staining of the SVZ in the vehicle control group and the EFV group. There was a strong trend for the EFV-treated group to have a lower Dcx expression level compared to the control group ($p = 0.08$). To uncover a possible underlying effect of EFV that may reduce the number of replicating NSCs in vivo, we measured apoptotic marker active caspase-3. Results indicated that EFV administration increased the number of active caspase-3-expressing cells in the SVZ compared to vehicle control-treated mice ($p < 0.05$) (Fig. 5C).

DISCUSSION

This study examines the effect of EFV on NSC proliferation in vitro and in vivo. Through in vitro experimentation with NSCs, we found that EFV resulted in a concentration-dependent

decrease in NSC proliferation beginning at a concentration of 5 μM by MTT assay (Fig. 1A). This was further confirmed by immunocytochemistry where EFV significantly reduced the incorporation of BrdU into NSCs as identified by nestin (Fig. 1B).

Our findings also indicated a concentration-dependent decrease in intracellular ATP as a result of EFV treatment of NSCs (Fig. 2A). Even though studies have shown that NSCs function at a lower metabolic rate when compared to other cells, a decreased level of intracellular NSC ATP can inhibit the overall process of NSC proliferation[39]. Recent studies have shown how various molecules that inhibit the actions of ATP, such as tricyclodecan-9-yl-xanthogenate (D609), decrease the rate of proliferation among NSCs, therefore opposing the process of proliferation[40]. Moreover in vitro results indicated that EFV lowered NSC MMP (Fig. 2B), an event associated with not only oxidative stress but also the initiation and activation of apoptosis[26,34,35].

LDH is a cytoplasmic enzyme that is released through damaged portions of the cellular membrane into the extracellular space[41]. The LDH assay has been shown to accurately measure cell death in vitro[42–45]. Increased levels of LDH among the NSCs treated with EFV (Fig. 3), as studied, are indicative of the apoptotic and/or necrotic effect of this drug on NSCs.

It has been reported that the p38 MAPK pathway and Bax are central to the negative regulation of proliferation of several cell types including stem cells[36,37]. This was shown in our study (Fig. 4) by an enhanced phosphorylation of p38 MAPK as well as upregulated Bax expression in EFV-stimulated NSCs. These data are in accordance with the observed reduced proliferation (Fig. 1), mitochondrial function (Fig. 2), and increased cell death (Fig. 3) imparted by EFV. Further, it is in agreement with other reports indicating that the increased reactive oxygen species (ROS), a result of reduced MMP[46], promote p38 MAPK phosphorylation[47], which in turn promotes Bax activation[38].

In addition to the in vitro treatment of NSCs, administration of EFV in vivo resulted in a decrease in NSC proliferation in C57BL/6J mice (Fig. 5). This was suggested by significantly decreased BrdU-positive cells in the SVZ (Fig. 5A). To examine whether the decreased BrdU staining that we observed in the SVZ of these mice reflected NSC commitment to the neuronal lineage, we also stained some sections with antibodies against Dcx, a neuronal lineage marker expressed in early stages of neuronal maturation[48,49]. Here we found a strong trend toward decreased Dcx expression nearing significance ($p = 0.08$) (Fig. 5B).

Since our in vitro studies showed increased cell death, cytotoxicity, and Bax expression imparted by EFV, we also stained for active caspase-3, which has previously been linked with loss of MMP[50]. We found a significant increase in active caspase-3 in the same region (Fig. 5C). Thus, our combined data suggest an inhibition of NSC proliferation in vitro and in vivo through induction of apoptosis, in effect leaving fewer cells present in the SVZ to divide as a result of EFV administration.

Regarding the role of EFV in neurodegeneration and survival of adult neurons, oral treatment of rats with EFV for 30 days promoted degenerative changes (decreased cellular

population, pyknotic nuclei, and presence of microcysts and edema) in the lateral geniculate body, suggesting a mechanistic action as a neurotoxin that disrupts cellular integrity[51]. Additionally, we demonstrated the ability of EFV to cause signs of neurodegeneration in mice in which pathologies characteristic of Alzheimer's disease (AD), such as increased brain β-secretase (BACE-1) expression and enhanced soluble amyloid-β (Aβ) generation, were observed[23]. Further, we found that EFV-treated SweAPP N2a neurons showed neurodegenerative signs in the form of mitochondrial dysfunction and upregulated BACE-1 expression, which promoted Aβ accumulation in this model of murine N2a cells transfected with human "Swedish" mutant amyloid precursor protein (APP)[23].

There is accumulating data pointing to an interference by EFV with CNS energy homeostasis and subsequent neurodegeneration. One investigation exploring this showed a significant inhibition of creatine kinase (CK) activity in the hippocampus, cerebellum, striatum, and cortex of mice treated with EFV[30]. CK is a catalyst for the transfer of the phosphoryl group from phosphocreatine to adenosine diphosphate (ADP) to regenerate ATP in the brain and other tissues that consume energy at a high rate. This reduced brain CK activity may partially be responsible for the cognitive impairments seen in EFV-treated mice, as suggested by the fact that knock-out mice for CK in the brain demonstrated cognitive impairment[52]. Importantly, results acquired from both animal[53] and human[54] studies have also correlated reduced CK activity with neurodegeneration. Additionally, it has been shown that treatment with EFV (10 or 25 μM) significantly decreased the viability of rat primary cortical neurons[20]. The neurodegenerative potential of the EFV metabolite 8-hydroxyefavirenz has also been shown in primary rat hippocampal neuronal cultures. In this model, 8-hydroxyefavirenz increased entry of extracellular Ca^{2+}, which was mediated largely by L-type voltage-gated calcium channels[55].

The SVZ is an important neurogenic niche, and neurons generated in the SVZ migrate along the rostral migratory stream to reach the olfactory bulb. Importantly, brain injuries stimulate SVZ direct migration of new NSCs to the sites of injury[56], which may compensate for some of the neurodegenerative changes promoted by EFV as noted above. NSCs can home similarly to pathologic sites in the brain arising from an array of etiologies[8]. It is thus possible that reduction of NSC proliferation in the SVZ due to EFV could contribute to a decline in regenerative actions of these cells, which under non-EFV conditions would oppose the chronic injury induced in the brain by HIV itself, HIV-activated glial cells, and/or the HIV-secreted proteins such as gp120 and Tat[57].

It is important to note that EFV has been linked to cognitive dysfunction in previous studies[16,18,19]. For example, Ciccarelli and colleagues found that EFV is associated with cognitive disorders even in asymptomatic HIV-infected patients[18]. Most recently it was also found clinically that long-term EFV treatment was associated with detriments to speed of information processing, verbal fluency, and working memory[16]. We speculate that EFV-mediated reductions of NSC proliferation may underlie some of these reported effects, although no studies to date have examined the exact relationship between reduced NSC proliferation and cognitive dysfunction specifically in EFV-treated HIV patients.

The current research has several strengths and weaknesses. Regarding the former, we observed consistent findings in both in vitro and in vivo model systems in that EFV causes decreased NSC proliferation. Additionally, we found the level of cellular oxidative stress (reduced ATP stores and MMP) imparted by EFV correlated consistently with reduced NSC proliferation and increased cytotoxicity, as well as p38 MAPK and Bax promotion at the 5 μM concentration. Second, our data coincide with other reports indicating that the process of NSC proliferation is highly sensitive to the redox balance in that cell proliferation is favored in more reduced environments, and cell differentiation is more favored in oxidized environments. As a result, as the levels of oxidative stress increase, the rate of proliferation decreases[58].

This report has limitations as well. First, it describes a potential mechanism for a subset of HAND cases since not all HIV-infected individuals are on EFV therapy. It should also be noted that, in the present study, we did not investigate the plasma or cerebrospinal fluid (CSF) concentrations of EFV or its metabolites in vivo. However, EFV has good CNS penetration[59], which could support the neurologic symptoms noted by others[16,18,19].

In sum, our present work suggests that EFV promotes a decrease in NSC proliferation, which is correlated with activation of oxidative stress pathways as well as Bax and active caspase-3 upregulation. It is in accordance with other reports indicating that oxidative stress promotes p38 MAPK phosphorylation[47], which in turn promotes Bax upregulation[38]. Together these data suggest that EFV is involved in negative regulation of NSC proliferation by reducing the number of existing NSCs that are available to divide and generate newborn cells. Given that oxidative stress correlated with the defects in NSCs, this study also lays the ground work for future experiments to identify possible antioxidant adjunctive treatments to be given with EFV that would promote protection of NSCs.

Acknowledgments

This research was supported by NIH/NIMH R01MH09873701 (B.G.), NIH/NCCIH R43AT008333 01A1 (B.G.), and the Florida High Tech Corridor Matching Grant Program (FHT 16-11) (B.G.). The authors declare no conflicts of interest.

References

1. Nath A, Sacktor N. Influence of highly active antiretroviral therapy on persistence of HIV in the central nervous system. Curr Opin Neurol. 2006; 19(4):358–61. [PubMed: 16914973]
2. Heaton RK, Franklin DR, Ellis RJ, McCutchan JA, Letendre SL, Leblanc S, Corkran SH, Duarte NA, Clifford DB, Woods SP, Collier AC, Marra CM, Morgello S, Mindt MR, Taylor MJ, Marcotte TD, Atkinson JH, Wolfson T, Gelman BB, McArthur JC, Simpson DM, Abramson I, Gamst A, Fennema-Notestine C, Jernigan TL, Wong J, Grant I. CHARTER GROUP, HNRC Group. HIV-associated neurocognitive disorders before and during the era of combination antiretroviral therapy: Differences in rates, nature, and predictors. J Neurovirol. 2011; 17(1):3–16. [PubMed: 21174240]
3. Ferrell D, Giunta B. The impact of HIV-1 on neurogenesis: Implications for HAND. Cell Mol Life Sci. 2014; 71(22):4387–92. [PubMed: 25134912]
4. Schwartz L, Civitello L, Dunn-Pirio A, Ryschkewitsch S, Berry E, Cavert W, Kinzel N, Lawrence DM, Hazra R, Major EO. Evidence of human immunodeficiency virus type 1 infection of nestin-positive neural progenitors in archival pediatric brain tissue. J Neurovirol. 2007; 13(3):274–83. [PubMed: 17613718]

5. Kaul M, Zheng J, Okamoto S, Gendelman HE, Lipton SA. HIV-1 infection and AIDS: Consequences for the central nervous system. Cell Death Differ. 2005; 12(Suppl 1):878–92. [PubMed: 15832177]

6. Schwartz L, Major EO. Neural progenitors and HIV-1-associated central nervous system disease in adults and children. Curr HIV Res. 2006; 4(3):319–27. [PubMed: 16842084]

7. Imitola J, Snyder EY, Khoury SJ. Genetic programs and responses of neural stem/progenitor cells during demyelination: Potential insights into repair mechanisms in multiple sclerosis. Physiol Genomics. 2003; 14(3):171–97. [PubMed: 12923300]

8. Imitola J, Park KI, Teng YD, Nisim S, Lachyankar M, Ourednik J, Mueller FJ, Yiou R, Atala A, Sidman RL, Tuszynski M, Khoury SJ, Snyder EY. Stem cells: Cross-talk and developmental programs. Philos Trans R Soc Lond B Biol Sci. 2004; 359(1445):823–37. [PubMed: 15293810]

9. Park KI, Ourednik J, Ourednik V, Taylor RM, Aboody KS, Auguste KI, Lachyankar MB, Redmond DE, Snyder EY. Global gene and cell replacement strategies via stem cells. Gene Ther. 2002; 9(10): 613–24. [PubMed: 12032707]

10. Park KI, Teng YD, Snyder EY. The injured brain interacts reciprocally with neural stem cells supported by scaffolds to reconstitute lost tissue. Nat Biotechnol. 2002; 20(11):1111–7. [PubMed: 12379868]

11. Snyder EY, Yoon C, Flax JD, Macklis JD. Multipotent neural precursors can differentiate toward replacement of neurons undergoing targeted apoptotic degeneration in adult mouse neocortex. Proc Natl Acad Sci USA. 1997; 94(21):11663–8. [PubMed: 9326667]

12. Aboody KS, Brown A, Rainov NG, Bower KA, Liu S, Yang W, Small JE, Herrlinger U, Ourednik V, Black PM, Breakefield XO, Snyder EY. Neural stem cells display extensive tropism for pathology in adult brain: Evidence from intracranial gliomas. Proc Natl Acad Sci USA. 2000; 97(23):12846–51. [PubMed: 11070094]

13. Rao VR, Ruiz AP, Prasad VR. Viral and cellular factors underlying neuropathogenesis in HIV associated neurocognitive disorders (HAND). AIDS Res Ther. 2014; 11:13. [PubMed: 24894206]

14. Del Guerra FB, Fonseca JL, Figueiredo VM, Ziff EB, Konkiewitz EC. Human immunodeficiency virus-associated depression: Contributions of immuno-inflammatory, monoaminergic, neurodegenerative, and neurotrophic pathways. J Neurovirol. 2013; 19(4):314–27. [PubMed: 23868513]

15. Fischer-Smith T, Rappaport J. Evolving paradigms in the pathogenesis of HIV-1-associated dementia. Expert Rev Mol Med. 2005; 7(27):1–26.

16. Ma QVF, Wong J, Sanders CA, Kao YT, Croteau D, Clifford DB, Collier AC, Gelman BB, Marra CM, McArthur JC, Morgello S, SImpson DM, Heaton RK, Grant I, Letendre SL. CHARTER Group. Long-term Efavirenz use is associated with worse neurocognitive functioning in HIV-infected patients. J Neurovirol. 2016; 22(2):170–8. [PubMed: 26407716]

17. AIDSinfo. Guidelines for the use of antiretroviral agents in HIV-1-infected adults and adolescents. 2016. Available from https://aidsinfo.nih.gov/guidelines/html/1/adult-andadolescent-treatment-guidelines/0

18. Ciccarelli N, Fabbiani M, Di Giambenedetto S, Fanti I, Baldonero E, Bracciale L, Tamburrini E, Cauda R, De Luca A, Silveri MC. Efavirenz associated with cognitive disorders in otherwise asymptomatic HIV-infected patients. Neurology. 2011; 76(16):1403–9. [PubMed: 21502598]

19. Romao PR, Lemos JC, Moreira J, de Chaves G, Moretti M, Castro AA, Andrade VM, Boeck CR, Quevedo J, Gavioli EC. Anti-HIV drugs nevirapine and efavirenz affect anxietyrelated behavior and cognitive performance in mice. Neurotox Res. 2011; 19(1):73–80. [PubMed: 20012242]

20. Funes HA, Apostolova N, Alegre F, Blas-Garcia A, Alvarez A, Marti-Cabrera M, Esplugues JV. Neuronal bioenergetics and acute mitochondrial dysfunction: A clue to understanding the central nervous system side effects of efavirenz. J Infect Dis. 2014; 210(9):1385–95. [PubMed: 24813473]

21. Sluis-Cremer N, Tachedjian G. Mechanisms of inhibition of HIV replication by non-nucleoside reverse transcriptase inhibitors. Virus Res. 2008; 134(1–2):147–56. [PubMed: 18372072]

22. Balzarini J. Current status of the non-nucleoside reverse transcriptase inhibitors of human immunodeficiency virus type 1. Curr Top Med Chem. 2004; 4(9):921–44. [PubMed: 15134549]

23. Brown LA, Jin J, Ferrell D, Sadic E, Obregon D, Smith AJ, Tan J, Giunta B. Efavirenz promotes beta-secretase expression and increased Abeta1-40,42 via oxidative stress and reduced microglial

phagocytosis: Implications for HIV associated neurocognitive disorders (HAND). PLoS One. 2014; 9(4):e95500. [PubMed: 24759994]

24. Chandra S, Murthy SN, Mondal D, Agrawal KC. Therapeutic effects of Nigella sativa on chronic HAART-induced hyperinsulinemia in rats. Can J Physiol Pharmacol. 2009; 87(4):300–9. [PubMed: 19370083]
25. Dragicevic N, Smith A, Lin X, Yuan F, Copes N, Delic V, Tan J, Cao C, Shytle RD, Bradshaw PC. Green tea epigallocatechin-3-gallate (EGCG) and other flavonoids reduce Alzheimer's amyloid-induced mitochondrial dysfunction. J Alzheimers Dis. 2011; 26(3):507–21. [PubMed: 21694462]
26. Naidu VGM, Atmakur H, Katragadda SB, Devabakthuni B, Kota A, SCK, Kuncha M, MVPSV, Kulkarni P, Janaswamy MR, Sistla R. Antioxidant, hepatoprotective and cytotoxic effects of icetexanes isolated from stem-bark of Premna tomentosa. Phytomedicine. 2014; 21(4):497–505. [PubMed: 24183951]
27. Dirson G, Fernandez C, Hindlet P, Roux F, German-Fattal M, Gimenez F, Farinotti R. Efavirenz does not interact with the ABCB1 transporter at the blood-brain barrier. Pharm Res. 2006; 23(7): 1525–32. [PubMed: 16779703]
28. Tohyama J, Billheimer JT, Fuki IV, Rothblat GH, Rader DJ, Millar JS. Effects of nevirapine and efavirenz on HDL cholesterol levels and reverse cholesterol transport in mice. Atherosclerosis. 2009; 204(2):418–23. [PubMed: 18990393]
29. Destache CJ, Belgum T, Goede M, Shibata A, Belshan MA. Antiretroviral release from poly(DL-lactide-co-glycolide) nanoparticles in mice. J Antimicrob Chemother. 2010; 65(10):2183–7. [PubMed: 20729545]
30. Streck EL, Scaini G, Rezin GT, Moreira J, Fochesato CM, Romao PR. Effects of the HIV treatment drugs nevirapine and efavirenz on brain creatine kinase activity. Metab Brain Dis. 2008; 23(4): 485–92. [PubMed: 18815873]
31. Gatch MB, Kozlenkov A, Huang RQ, Yang W, Nguyen JD, Gonzalez-Maeso J, Rice KC, France CP, Dillon GH, Forster MJ, Schetz JA. The HIV antiretroviral drug efavirenz has LSD-like properties. Neuropsychopharmacology. 2013; 38(12):2373–84. [PubMed: 23702798]
32. Bachstetter AD, Jernberg J, Schlunk A, Vila JL, Hudson C, Cole MJ, Shytle RD, Tan J, Sanberg PR, Sanberg CD, Borlongan C, Kaneko Y, Tajiri N, Gemma C, Bickford PC. Spirulina promotes stem cell genesis and protects against LPS induced declines in neural stem cell proliferation. PLoS One. 2010; 5(5):e10496. [PubMed: 20463965]
33. Park D, Xiang AP, Mao FF, Zhang L, Di CG, Liu XM, Shao Y, Ma BF, Lee JH, Ha KS, Walton N, Lahn BT. Nestin is required for the proper self-renewal of neural stem cells. Stem Cells. 2010; 28(12):2162–71. [PubMed: 20963821]
34. Gottlieb E, Armour SM, Harris MH, Thompson CB. Mitochondrial membrane potential regulates matrix configuration and cytochrome c release during apoptosis. Cell Death Differ. 2003; 10(6): 709–17. [PubMed: 12761579]
35. Susin SA, Lorenzo HK, Zamzami N, Marzo I, Snow BE, Brothers GM, Mangion J, Jacotot E, Costantini P, Loeffler M, Larochette N, Goodlett DR, Aebersold R, Siderovski DP, Penninger JM, Kroemer G. Molecular characterization of mitochondrial apoptosis-inducing factor. Nature. 1999; 397(6718):441–6. [PubMed: 9989411]
36. Hadjal Y, Hadadeh O, Yazidi CE, Barruet E, Binetruy B. A p38MAPK-p53 cascade regulates mesodermal differentiation and neurogenesis of embryonic stem cells. Cell Death Dis. 2013; 4:e737. [PubMed: 23887628]
37. Su P, Zhang J, Zhao F, Aschner M, Chen J, Luo W. The interaction between microglia and neural stem/precursor cells. Brain Res Bull. 2014; 109:32–8. [PubMed: 25245208]
38. Ghatan S, Larner S, Kinoshita Y, Hetman M, Patel L, Xia Z, Youle RJ, Morrison RS. p38 MAP kinase mediates bax translocation in nitric oxide-induced apoptosis in neurons. J Cell Biol. 2000; 150(2):335–47. [PubMed: 10908576]
39. Huang TT, Zou Y, Corniola R. Oxidative stress and adult neurogenesis—Effects of radiation and superoxide dismutase deficiency. Semin Cell Dev Biol. 2012; 23(7):738–44. [PubMed: 22521481]
40. Kalluri HS, Dempsey RJ. D609-mediated inhibition of ATP synthesis in neural progenitor cells. Neuroreport. 2014; 25(10):777–81. [PubMed: 24918458]

41. Chan FK, Moriwaki K, De Rosa MJ. Detection of necrosis by release of lactate dehydrogenase activity. Methods Mol Biol. 2013; 979:65–70. [PubMed: 23397389]
42. Uchide N, Ohyama K, Bessho T, Toyoda H. Lactate dehydrogenase leakage as a marker for apoptotic cell degradation induced by influenza virus infection in human fetal membrane cells. Intervirology. 2009; 52(3):164–73. [PubMed: 19521105]
43. Koh JY, Cotman CW. Programmed cell death: Its possible contribution to neurotoxicity mediated by calcium channel antagonists. Brain Res. 1992; 587(2):233–40. [PubMed: 1525659]
44. Koh JY, Gwag BJ, Lobner D, Choi DW. Potentiated necrosis of cultured cortical neurons by neurotrophins. Science. 1995; 268(5210):573–5. [PubMed: 7725105]
45. Gwag BJ, Lobner D, Koh JY, Wie MB, Choi DW. Blockade of glutamate receptors unmasks neuronal apoptosis after oxygen-glucose deprivation in vitro. Neuroscience. 1995; 68(3):615–9. [PubMed: 8577361]
46. Tang XQ, Feng JQ, Chen J, Chen PX, Zhi JL, Cui Y, Guo RX, Yu HM. Protection of oxidative preconditioning against apoptosis induced by H_2O_2 in PC12 cells: Mechanisms via MMP, ROS, and Bcl-2. Brain Res. 2005; 1057(1–2):57–64. [PubMed: 16129420]
47. Wang X, Luo F, Zhao H. Paraquat-induced reactive oxygen species inhibit neutrophil apoptosis via a p38 MAPK/NFkappaB-IL-6/TNF-alpha positive-feedback circuit. PLoS One. 2014; 9(4):e93837. [PubMed: 24714343]
48. Francis F, Koulakoff A, Boucher D, Chafey P, Schaar B, Vinet MC, Friocourt G, McDonnell N, Reiner O, Kahn A, McConnell SK, Berwald-Netter Y, Denoulet P, Chelly J. Doublecortin is a developmentally regulated, microtubuleassociated protein expressed in migrating and differentiating neurons. Neuron. 1999; 23(2):247–56. [PubMed: 10399932]
49. Gleeson JG, Lin PT, Flanagan LA, Walsh CA. Doublecortin is a microtubule-associated protein and is expressed widely by migrating neurons. Neuron. 1999; 23(2):257–71. [PubMed: 10399933]
50. Meeran SM, Katiyar SK. Grape seed proanthocyanidins promote apoptosis in human epidermoid carcinoma A431 cells through alterations in Cdki-Cdk-cyclin cascade, and caspase-3 activation via loss of mitochondrial membrane potential. Exp Dermatol. 2007; 16(5):405–15. [PubMed: 17437483]
51. Adjene JO, Igbigbi PS, Nwose EU. Histological effects of chronic administration of efavirenz on lateral geniculate body of adult Wistar rats. N Am J Med Sci. 2010; 2(1):1–4. [PubMed: 22624105]
52. Jost CR, Van Der Zee CE, In't Zandt HJ, Oerlemans F, Verheij M, Streijger F, Fransen J, Heerschap A, Cools AR, Wieringa B. Creatine kinase B-driven energy transfer in the brain is important for habituation and spatial learning behaviour, mossy fibre field size and determination of seizure susceptibility. Eur J Neurosci. 2002; 15(10):1692–706. [PubMed: 12059977]
53. Wendt S, Dedeoglu A, Speer O, Wallimann T, Beal MF, Andreassen OA. Reduced creatine kinase activity in transgenic amyotrophic lateral sclerosis mice. Free Radic Biol Med. 2002; 32(9):920–6. [PubMed: 11978494]
54. Aksenov M, Aksenova M, Butterfield DA, Markesbery WR. Oxidative modification of creatine kinase BB in Alzheimer's disease brain. J Neurochem. 2000; 74(6):2520–7. [PubMed: 10820214]
55. Tovar-y-Romo LB, Bumpus NN, Pomerantz D, Avery LB, Sacktor N, McArthur JC, Haughey NJ. Dendritic spine injury induced by the 8-hydroxy metabolite of efavirenz. J Pharmacol Exp Ther. 2012; 343(3):696–703. [PubMed: 22984227]
56. Saha B, Peron S, Murray K, Jaber M, Gaillard A. Cortical lesion stimulates adult subventricular zone neural progenitor cell proliferation and migration to the site of injury. Stem Cell Res. 2013; 11(3):965–77. [PubMed: 23900166]
57. Giunta B, Obregon D, Hou H, Zeng J, Sun N, Nikolic V, Ehrhart J, Shytle D, Fernandez F, Tan J. EGCG mitigates neurotoxicity mediated by HIV-1 proteins gp120 and Tat in the presence of IFN-gamma: Role of JAK/STAT1 signaling and implications for HIV-associated dementia. Brain Res. 2006; 1123(1):216–25. [PubMed: 17078933]
58. Schafer FQ, Buettner GR. Redox environment of the cell as viewed through the redox state of the glutathione disulfide/glutathione couple. Free Radic Biol Med. 2001; 30(11):1191–212. [PubMed: 11368918]

59. Wynn HE, Brundage RC, Fletcher CV. Clinical implications of CNS penetration of antiretroviral drugs. CNS Drugs. 2002; 16(9):595–609. [PubMed: 12153332]

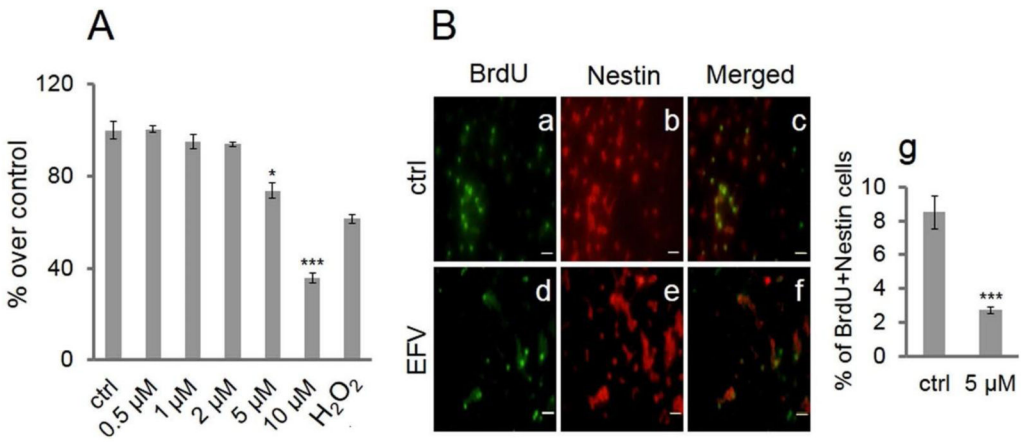

Figure 1.

Efavirenz (EFV) reduces proliferation of neural stem cells (NSCs). EFV reduces proliferation of NSCs by MTT assay. (A) NSCs were treated with a series of concentrations of EFV, vehicle control (ctrl), and H_2O_2 (positive control; 100 μM) for 24 h. Data are presented as a percentage of EFV treatment over ctrl. Each bar is presented as mean ± SEM (*$p < 0.05$; ***$p < 0.001$). (B) EFV inhibits bromodeoxyuridine (BrdU) incorporation into NSCs as evidenced by immunocytochemistry: After treatment consisting of 5 μM of EFV or vehicle control (ctrl) for 24 h, and incubation with BrdU (10 μM) for 2 h, NSCs were fluorescence stained with BrdU (green) and nestin (red). Staining of control treatment is shown in (a) BrdU, (b) nestin, and (c) merged; EFV treatment in (d) BrdU, (e) nestin, and (f) merged. Scale bars: 20 μm (a–f). (g) Quantified data are expressed as the percentage of double-labeled cells. Data are presented as mean ± SEM (***$p < 0.001$).

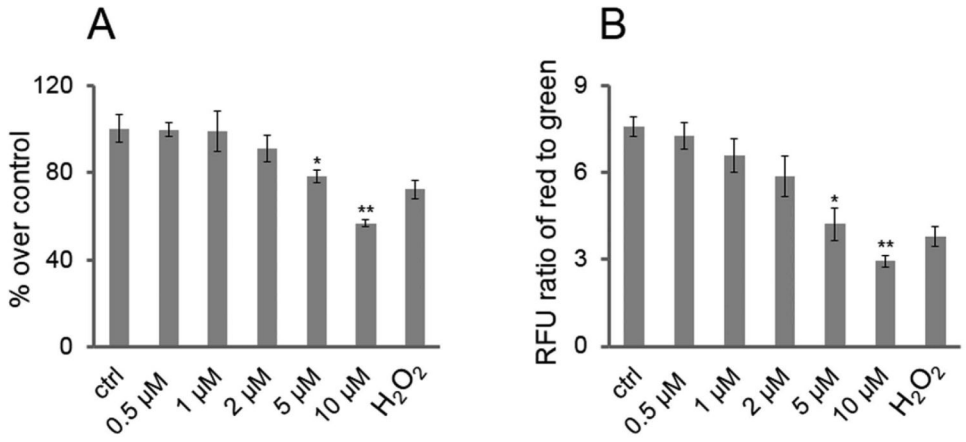

Figure 2.

EFV reduces NSC adenosine triphosphate (ATP) stores and mitochondrial membrane potential (MMP). (A) EFV reduces NSC ATP stores: NSCs were plated in 12-well plates with 3×10^5 cells per well and treated with a series of concentrations of EFV, vehicle control (ctrl), and H_2O_2 (positive control; 100 μM) for 24 h. The relevant luminescence units (RLU) were measured for each condition. The percentages of treatment over ctrl represents intracellular ATP levels of NSCs. Each bar is presented as mean ± SEM (*$p < 0.05$; **$p < 0.01$). (B) EFV reduces MMP of NSCs: After NSCs were treated with a series of concentrations of EFV, vehicle control (ctrl), and H_2O_2 (positive control; 100 μM) for 6 h, they were incubated with JC-1 to detect MMP. The ratio of red fluorescence (RFU) to green fluorescence (RFU) represents the value of MMP. Data are presented as mean ± SEM (*$p < 0.05$; **$p < 0.01$).

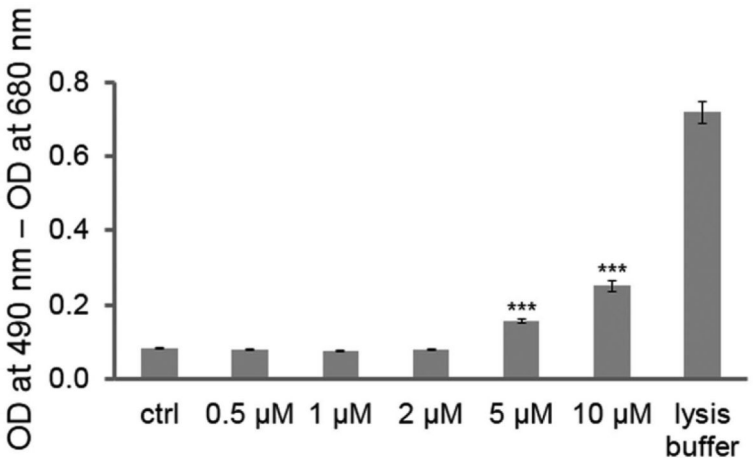

Figure 3.

EFV increases NSC cytotoxicity and cell death. EFV induces increased cell death of NSCs in a dose-dependent manner. Cells were treated with a series of dilutions of EFV, vehicle control (ctrl), or assay-positive control (10% cell lysis buffer) for 24 h, and cell culture media were subjected to an LDH assay. The value of optical density (OD) at 490 nm subtracted from the value of OD at 680 nm represents LDH levels. Data are presented as mean ± SEM (***$p < 0.001$).

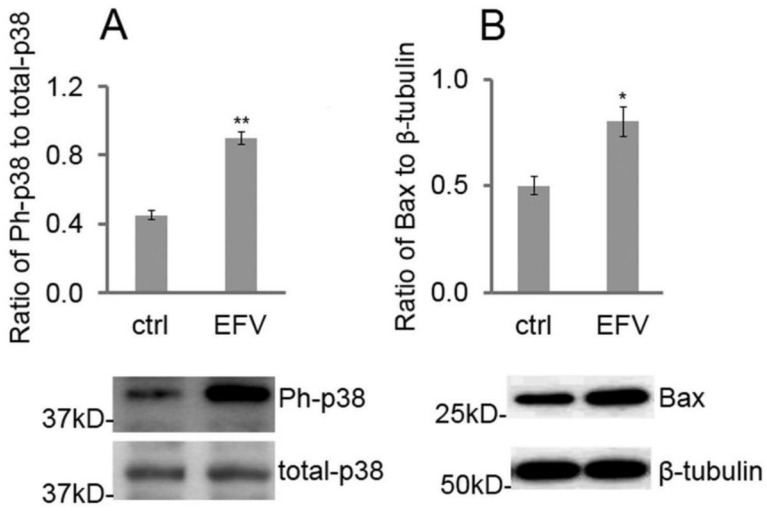

Figure 4.

EFV increases p38 MAPK phosphorylation and Bax expression. (A) EFV elevates the expression of phospho-p38 in NSCs detected by Western blot. NSCs were plated in 24-well plates for 24 h, treated with 5 μM of EFV or vehicle control (ctrl) for 1 h. Cells were then lysed and subjected to Western blot of phospho-p38 (Ph-p38) and total p38. Each bar is presented as mean ± SEM (**$p < 0.01$). (B) EFV elevates expression of Bax from NSCs. To detect Bax expression, cells were treated for 24 h with 5 μM of EFV or vehicle control (ctrl). Data are presented as mean ± SEM (*$p < 0.05$).

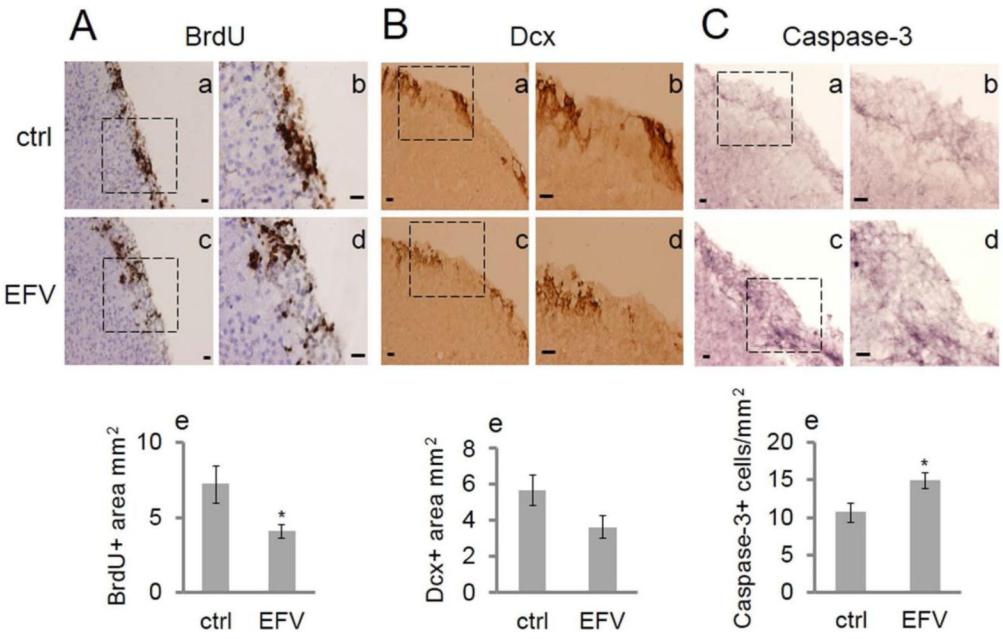

Figure 5.

EFV administration impairs NSC proliferation and induces apoptosis in the SVZ. (A) Administration of EFV (20 mg/kg) impairs BrdU incorporation in the SVZ of C57BL/6J mice. Mice were administered daily IP injections of EFV or vehicle control (ctrl) for 4 weeks and BrdU administration for 5 consecutive days prior to euthanization. Sagittal sections were stained with BrdU antibody. (a, b) The square marked in (a) represents the vehicle control (ctrl)-treated group and is magnified in (b) ($n = 7$); (c) and (d) the square marked in (c) represents EFV treated group and is magnified in (d) ($n = 8$). Scale bar: 20 μm (in micrographs). (e) Quantitative data are represented by the bar graph. Each bar is presented as mean ± SEM (*$p < 0.05$). (B) Administration of EFV shows a trend to decrease Dcx expression in C57BL/6J mice in the SVZ. Sagittal sections from the same mice were stained by Dcx antibody. (a, b) The square marked in (a) represents the vehicle control (ctrl) group and is magnified in (b) ($n = 7$). (c, d) The square marked in (c) represents the EFV treatment group and is magnified in (d) ($n = 8$). Scale bars: 20 μm (in micrographs). (e) Quantitative data are represented in the bar graph. Each bar is presented as mean ± SEM ($p = 0.08$). (C) Administration of EFV enhances active caspase-3 expression in the SVZ. Sagittal sections from the same mice were stained by active caspase-3 antibody to evaluate apoptosis in the SVZ of C57BL/6J mice. (a, b) The square marked in (a) represents the vehicle control (ctrl) group and is magnified in (b) ($n = 7$). (c, d) The square in (c) represents the EFV treatment group ($n = 8$) and is magnified in (d). Scale bars: 20 μm (in micrographs). (e) Quantitative data are represented in the bar graph. Data are presented as mean ± SEM (*$p < 0.05$).